Volume 12, Number 3, 2019. pp. 209-221

Jordan Journal of Physics

ARTICLE

Simulation-Assisted Environment-Mapping Using Unidirectional Ultrasonic Pulses

M. Al-Shorman[a], **M. Al-Kofahi**[b] and **Q. I. Mohaidat**[a]

[a] *Department of Physics. Yarmouk University. Irbid, Jordan.*

[b] *Department of Computer Information Science, Higher College of Technology, Ras Al-Khaimah, UAE.*

Received on: 30/9/2018; Accepted on: 17/3/2019

Abstract: In this paper, a new system for mapping and discovering an environment using simple ultrasound transceivers, connected to a microcontroller, is developed with the aid of an ultrasonic wavelet propagation simulation program. Environment mapping is achieved by sending ultrasonic pulses with known characteristics and listening to the reflections from all directions in real time. The change induced in the shape of a pulse wavefront due to reflection is found to be dependent on the barriers in the environment and on its geometry. The correlation between the changes in the shapes of the wavefronts and the shapes of the reflecting objects is investigated. This includes the slope or curvature of the reflecting wall (or barrier), wall tilt or angle and possible twists in corners. By analyzing the interference patterns and counting the interference fringes in the reflected pulses, a method for measuring object orientation is developed. The presented technique can also discover unseen objects behind corners. The results obtained show that this method is not only effective in discovering an environment, but also in measuring subtle features, such as the rotation of an object with an accuracy of 0.1°. The mapping and discovery techniques described in this paper are targeted for artificial intelligence applications and robotics. The infinite number of possibilities in the reflected wavefront characteristics, due to the similarly infinite environment shapes, makes experimentally collecting this data impossible. The simulated data presented in this paper will take more than six months to be collected experimentally.

Keywords: Simulation, Environment mapping, Unidirectional ultrasonic pulses.

Introduction

Several strategies have been used to obtain an environment's features using ultrasonic sensors due to their low cost and simplicity. Mapping and navigating an environment can be very useful in many applications.

Recent advances in navigation range from navigating wheel chairs [1] to vehicles [2] or any robot in general [3, 4, 5, 6]. For example, the authors in [7, 8] used signals from a set of distributed ultrasonic sensors to locate obstacles in 3D to help navigate a robot.

Mapping applications range from small features and cavities [9, 10, 11] to larger areas for robot and vehicle navigation [12, 13, 14]. The most common mapping technique is based on the time elapsed between transmission and reception of a pulse. Efforts in this field, using sound and ultrasound, varied from trying to distinguish a wall from a corner [6] or poles from trees [16], to the more elaborate efforts [17, 18, 19] of estimating a room geometry using omni-directional loudspeakers and multiple non-matched omni-directional microphones, located

Corresponding Author: M. Al-Shorman **Email**: shormanm@yu.edu.jo

randomly in the room. In these studies [17, 18], a room with different walls has been successfully described by using first-order echoes collected by microphones. However, the fact that microphones had to be scattered in a room made the technique less applicable for robotics applications. Besides, this imposed some limits on the shape of the environment.

The authors in [20, 21] introduced an active sensing technique that allows to estimate the number of occupants by detecting the changes in a room's acoustic properties. In their study, a centrally located beacon transmits an ultrasonic chirp and then records how the signal dissipates over time. By analyzing the frequency response over the chirp's bandwidth at a few known occupancy levels, they are able to extrapolate the response as the number of people in the room changes.

Contribution

In this paper, a new method for mapping and discovering an unknown environment using *unidirectional* ultrasonic pulses, without imposing any limitation on the unknown environment shape, is presented. The new method works by extracting simple characteristics from the reflected wavefronts and relating the changes in those characteristics to previously studied surface properties. Features, such as a wall tilt/slope, an angle magnitude and pointing direction or a wall curvature, can be measured easily in less than a second. More complicated tasks, such as measuring the dimensions of a room without having a direct line of sight and detecting objects hiding behind an angle, are also possible. A new method for measuring object rotation by observing ultrasound interference patterns to an accuracy of 0.1° using 40kHz transmitter is introduced. This 0.1° accuracy can be enhanced even more by using a higher frequency transmitter. The new mapping method is targeted for compact and low-power devices, such as robots that operate on batteries, because of the low processing power needed to extract the intended wavefront features. The new method is also ideal for artificial intelligence applications, where a robot/machine can learn to discover an environment by observing a specific set of features in the reflected wavefronts.

Since collecting experimental data for the vast number of possible environment shapes under study is not practical, an ultrasound propagation simulator was developed and used. The developed simulator was tested and validated rigorously [22].

Unlike previous environment mapping attempts, the set of transceivers used were all mounted on the same device within few centimeters from each other, rather than being scattered in a room. Although it is possible to use regular sound waves for this application, ultrasound waves are preferred, because they are silent to the human ear and give a better spatial resolution compared to sound waves due to their shorter wavelengths. Ultrasound waves also have the advantage of being less prone to background noise.

This paper is organized as follows: A brief description of the simulation program used will be given. Then, the mapping technique will be described. Next, some mapping scenarios ranging from measuring an angle to seeing hidden objects behind a corner will be discussed. Finally, a conclusion will be given and some future work will be discussed.

Ultrasound Pulse Simulator

The simulator program has two main software components: A front-end written in C# and C++ that is responsible for parsing and interpreting the user input and a back-end that runs the actual simulation kernel written using OpenCL 2.0 heterogeneous compute language. OpenCL code can be run on a regular CPU or on a Graphics Processing Unit (GPU). GPUs have the advantage of typically containing several thousand compute units, while CPUs contain only few cores. This makes GPUs ideal for some computational tasks that can be massively parallelized. In this simulator, it is assumed that a pulse consists of millions of wavelets. The simulation of each wavelet runs on a separate compute unit on the GPU. Each wavelet oscillates and moves independently according to the equation:

$$r(\vec{t}) = \frac{A_0}{r} sin(kx - wt)\hat{r} \tag{1}$$

Once a wavelet hits a wall, it will change its direction such that the incidence angle equals the reflection angle. There is no limitation on the shape and number of walls in the simulated environment. Surface roughness and scattering are ignored.

The simulator models the following environment components:

- Walls and obstacles: All physical obstacles are assumed to be homogeneous. Scattering and surface roughness are ignored. All wall shapes are described inside the simulation using mathematical formulae that are not limited by shape or number. More complicated features can be described using a series of small linear segments.
- Ultrasonic pulse with known shape and properties: Throughout this work, a 40 kHz conic-shaped pulse that models the one generated by the commonly used, low cost HC-SR04 transceiver, is used. A pulse is assumed to consist of a large number of wavelets that are evenly spaced in the radial and angular directions. The chosen wavelet density should balance the accuracy against the simulation performance. During our tests, a $0.02^{\circ}-0.001^{\circ}$ angular spacing and a 1.0 mm radial spacing produced good results over a distance of $3-5$ meters. The emitted pulse spatial intensity profile is assumed to be Gaussian in the radial and angular directions. Full-width at half-maximum (FWHM), in the radial and angular directions, values of R_{FWHM} = 30*mm* and $\Theta_{FWHM} = 60^{\circ}$ were found to be a good match for HC-SR04 emitted pulse. See Fig. 4.
- Ultrasound receivers: A receiver is simulated as a region in space that records the passing wavelet amplitude, at its location, as a function of time. The recorded intensity is proportional to the receiver effective-area facing the incident wavelet. Each receiver has a known location, width and orientation. At the end of a simulation run, each receiver will have an intensity-time profile that resulted from a large number of wavelets crossing its location at different times. In this work, a typical simulation run modeled 360 receivers arranged in a 10cm-radius circle.

To demonstrate the accuracy of the simulation, a 78.5° corner was setup and twisted 2.5° counterclockwise. This arrangement will cause the incident pulse to have three separate wavefronts once reflected. The asymmetric shape of this arrangement means that the three wavefronts will not be similar and each one of them is expected to have a different intensity and space-time location. As shown in Fig. 3, the positions, shapes and relative intensities in the experimental data are the same as those in the simulated data.

How the Mapping Process Works

The three main components of the mapping device, shown in Fig. 1 as a 3D model, are:

Transmitter: To map an environment using the proposed technique, an ultrasound transmitter that can send a 1 μs to 100 μs pulse in a known direction is needed. The transmitted pulse must have a known intensity spatial distribution. The transmitter characteristics, such as the angular spread of the transmitted pulse, must be known. The transmitter should be located at the center of a circular array of receivers. Fig. 4 shows a simulated pulse spatial distribution similar to the used 40kHz HC-SR04 transceiver pulse. This transceiver works by applying $\pm 15V$ voltage pulses on its piezoelectric element. The colors in Fig. 4 represent the normalized intensity using the color scale shown to the right of the figure.

Receiver Array: Once a pulse is transmitted, a set of receivers packed in a circle, as tightly as possible, start recording the reflected intensity in real time. A sampling rate of 0.5 Mega Sample Per Second (0.5 MSPS) was sufficient during our tests. A circle of 10*cm* radius can pack about 360 2.5 *mm*-width receivers. Instead of building this large set of receivers, a smaller rotating set can do the same job albeit in a longer period of time. The data collected from this large set of receivers, as a function of time, is plotted on a two-dimensional color map, where intensity is represented by the color. The normalized intensity color scale used is shown to the right of each plot throughout this paper.

Microcontroller: The transmitter and the receiver array must be connected to a microcontroller (MCU) or a field programmable gate array (FPGA) that can handle all of the analog signals in real time. An Atmel SAM3X8E ARM CortexM3 MCU was sufficient when the receiver is attached to Wantai 42BYGHM809 stepper motor (400 steps/rev) and its generic M542H driver.

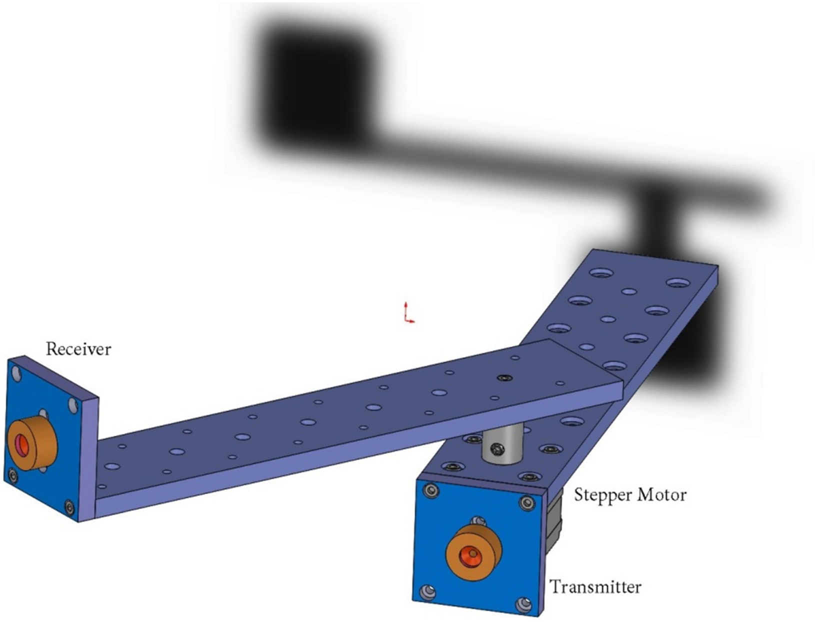

FIG. 1. Experimental setup 3D model.

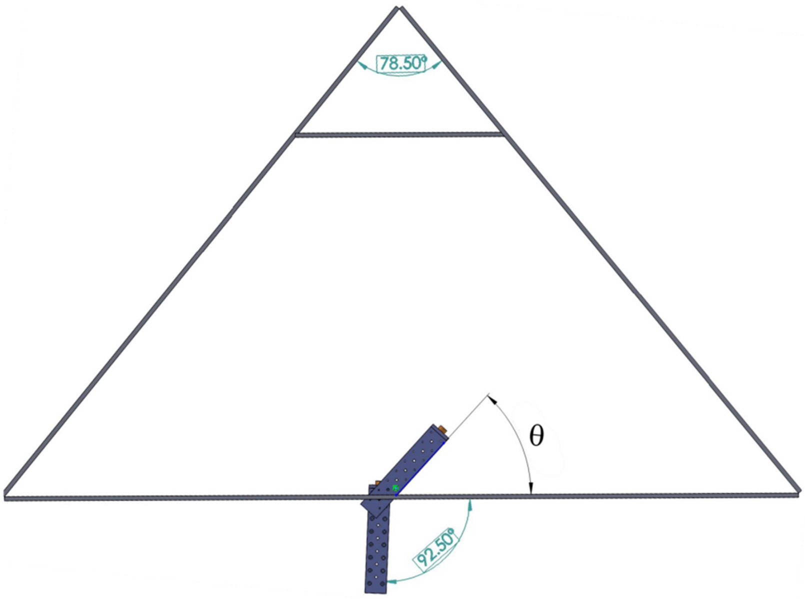

FIG. 2. Environment walls used to collect the experimental and simulated data shown in Fig. 3.

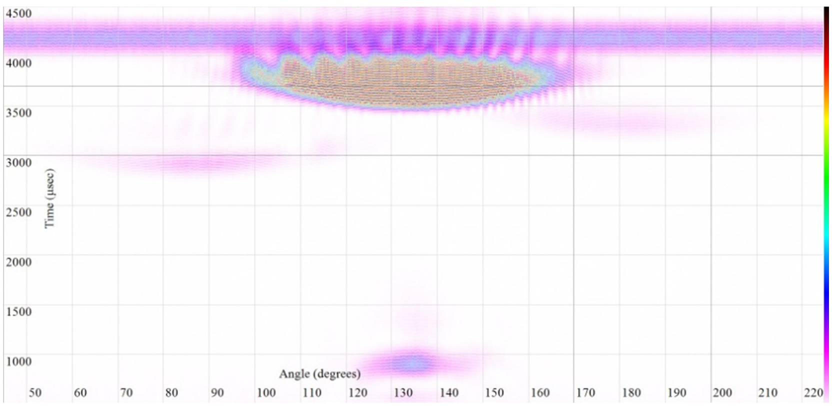

(a) Experimental

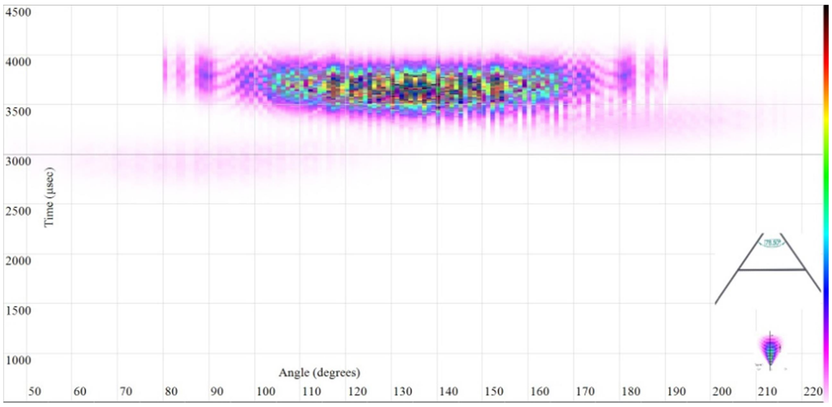

(b) Simulated

FIG. 3. Experimental *vs*. simulated ultrasound propagation data. The environment in which the pulse is propagating is shown in the inset of Fig. 3b and Fig. 2. The corner angle is 78.5° and is twisted 2.5°. X-axis: detector angle in degrees. Y-axis: time in micro-seconds. The normalized intensity is represented by the color scale to the right of each figure.

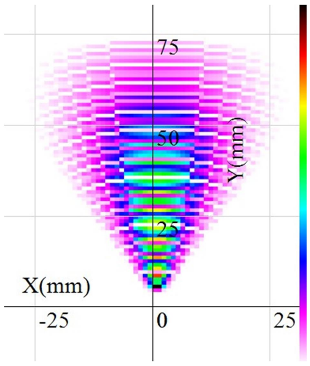

FIG. 4. A simulated 40kHz ultrasonic pulse spatial distribution similar to HC-SR04 transceiver pulse. X- & Y-axes: distance in millimeters.

Mapping Criteria

An environment can be mapped by tracking changes to the reflected pulse. For example, a reflected pulse may:

- Change its angular spread.
- Change its time spread.
- Get separated into two overlapping/non-overlapping wavefronts.
- Contain wave interference patterns.
- Include a specific object signature.

It should be emphasized here that:

- A direct line of sight is not necessary.
- A pulse may undergo multiple reflections before going back to the receivers.
- The direction from which a reflected pulse comes is not necessarily the original transmission direction.

Mapping Scenarios

This section discusses how to infer an environment characteristic from the reflected wavefront properties. Those characteristics can be as simple as a wall slope or as complicated as detecting an unseen object behind an angle.

Measuring a Wall Slope and Curvature

This section demonstrates how to use one of the reflected wavefront properties, its center, to calculate the slope of a wall. When a uniform pulse, such as the one shown in Fig. 4, direction of incidence is perpendicular to a wall, the reflected wavefront will come back to the direction from which it originated. The reflected wavefront will look like the reflection shown in Fig. 5a. Note that the x-axis in Fig. 5 is the detector angular position. The wavefront center in Fig. 5a, at 90°, is the original pulse incidence direction.

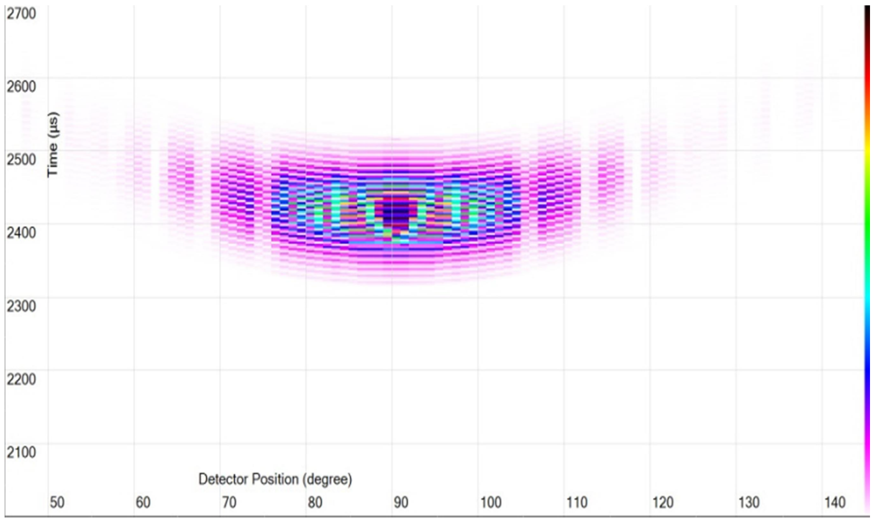

(a) Normal incidence

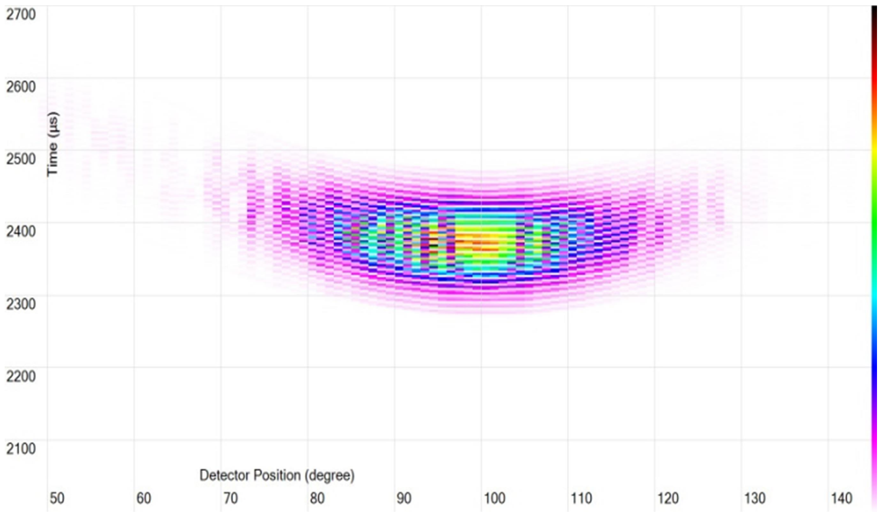

(b) 10° deviation from normal incidence.

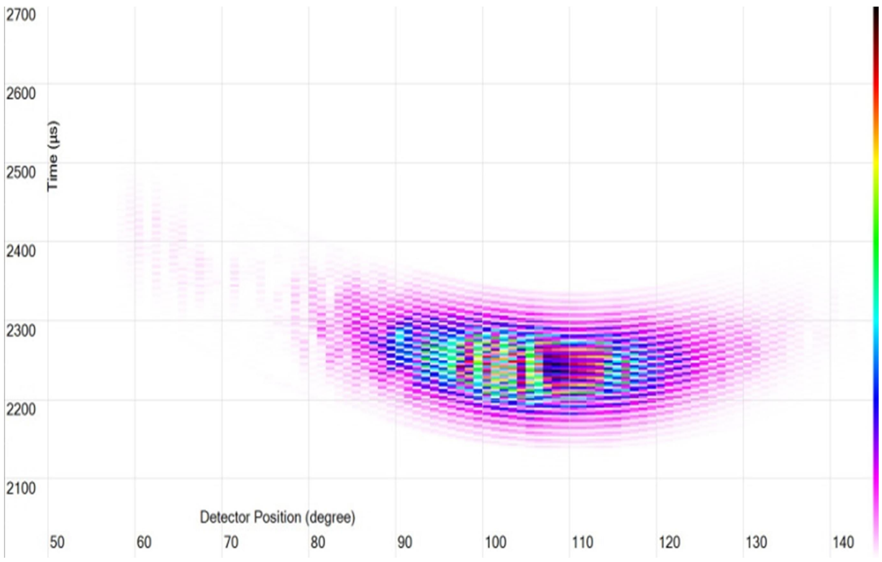

(c) 20° deviation from normal incidence.

FIG. 5. Reflected wavefront for various incidence angles. X-axis: detector angle in degrees. Y-axis: time in micro-seconds. The normalized intensity is represented by the color scale to the right of each figure.

If the angle between the incident pulse direction and the wall surface starts deviating from 90°, the reflected wavefront shape will deviate from the symmetric shape. For example, Figs. 5b and 5c show the reflected wavefront if the angles between the direction of incidence and the normal to the wall are 10° and 20°, respectively. This deviation can be quantified by either integrating the reflected wavefront intensity over time (y-axis) or integrating it over detector angular position (x-axis) and then comparing the result with normal incidence. Fig. 6a shows time-integrated intensity *vs*. detector angular position for various wall pointing directions. Note how the position of the peaks changes with the wall pointing direction. A large set of curves, as the ones shown in Fig. 6a, are put together in Fig. 6b. Each vertical slice from Fig. 6b represents a curve similar to the ones shown in Fig. 6a. The estimated maximum error in measuring the slope of a wall using this technique is about 4%.

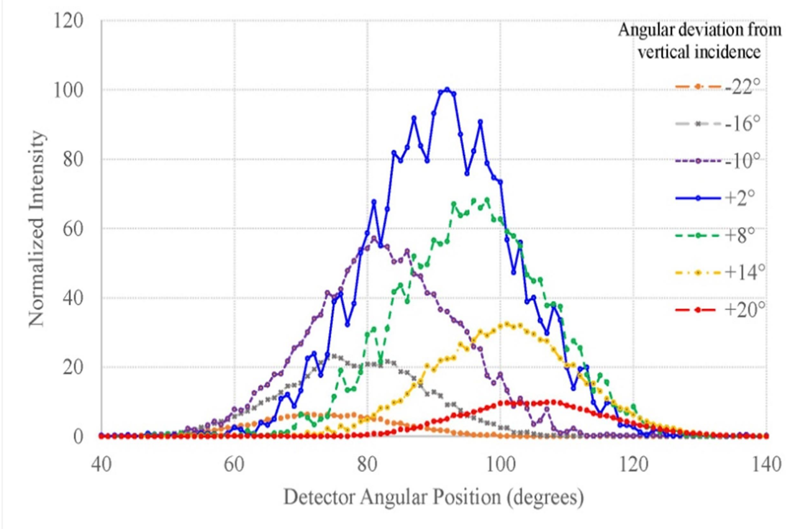

(a) Time-integrated intensity *vs*. detector position for different wall pointing directions. A wall direction is the angle between the normal to the surface and the incidence angle.

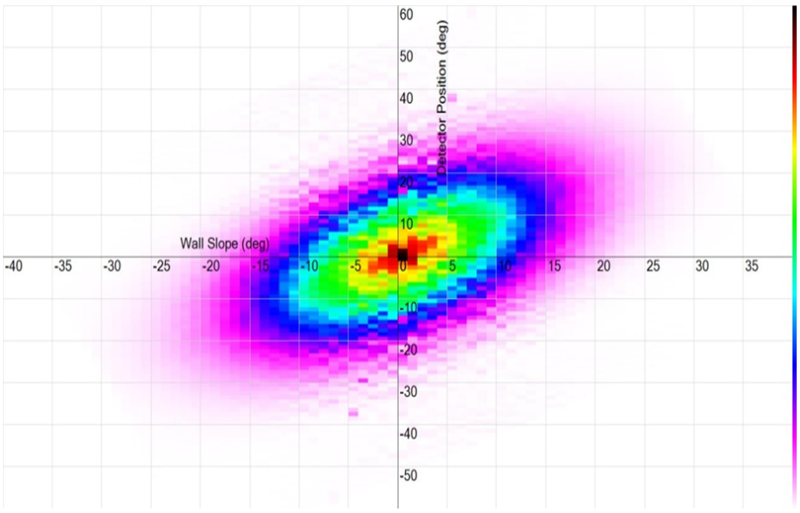

(b) Wall pointing direction *vs*. detector position. The color represents the normalized intensity. The intensity color scale is shown to the right. X-axis: wall slope in degrees. Y-axis: detector position in degrees.

FIG. 6. A pulse reflected from a wall will have its position shifted by an amount that depends on the wall pointing direction.

Another property of the reflected wavefront is its width. Fig. 7 shows the final result of how this property can be used to calculate a wall curvature. The same technique can be applied for walls/corners that cannot be seen directly by measuring reflections from a known plane wall. Discovered walls can be used as mirrors to see other objects by observing the change in a reflected wavefront position and width.

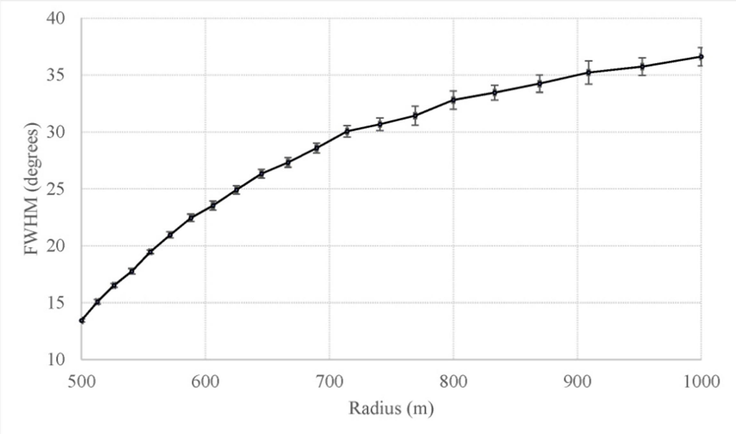

FIG. 7. Wall curvature measurement: FWHM of reflected wavefront time-integrated intensity *vs*. curvature radius.

Measuring an Angle

When a pulse gets reflected from a corner, the incident wavefront will get split into two wavefronts. The reflected wavefront time-integrated-intensity *vs*. detector angular position is shown in Fig. 8a for various angles. Note how interference patterns start forming once the two reflected wavefronts start overlapping. When the interference patterns are not the dominant feature of the reflected wavefront, the separation between the two peaks can be used as a metric to measure the wall angle. However, when the interference patterns are very strong, the spacing between the interference fringe separation and their number can be used as a metric for measuring the angle. See Fig. 8b.

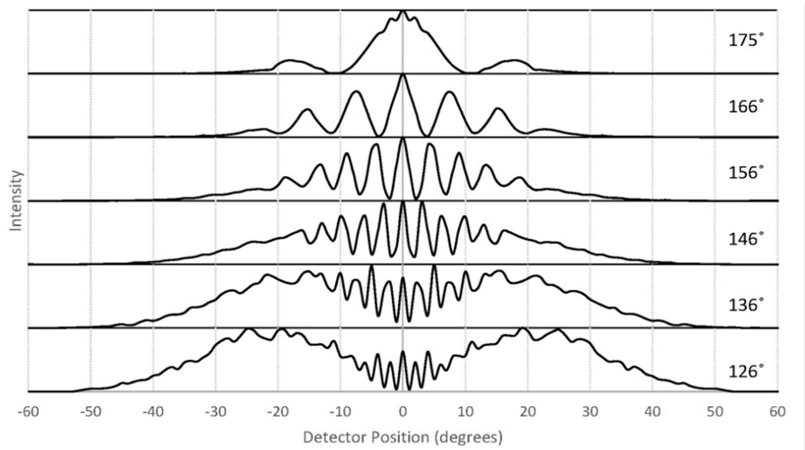

(a) Time-integrated intensity *vs*. detector angular position of a pulse reflected from a corner.

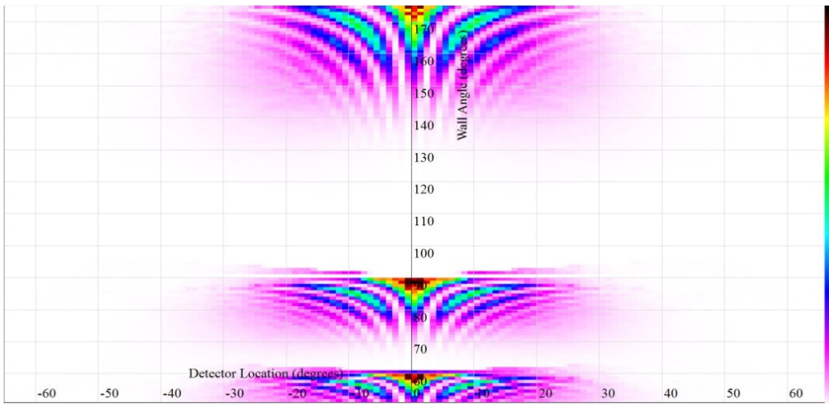

(b) A large number of curves, such as the curves in Fig. 8a, for a wide range of wall angles, are packed together to give time-integrated intensity *vs*. detector-location *vs*. wall angle. X-axis: detector location in degrees. Y-axis: wall direction in degrees.

FIG. 8. Effect of a corner on the shape of a reflected wavefront.

Measuring an Angle Twist

If the incident pulse does not divide a corner into halfes, the two reflected wavefronts will not be symmetric. This will result in either two separate wavefronts with different angular locations and relative intensities, as in Fig. 9, or two overlapping wavefronts with strong interference patterns, as in Fig. 10.

The strong interference patterns shown in Fig. 10 can be useful, not only in mapping an area, but also in positioning objects. For example, a tiny angular object can be mounted on a plane surface that needs to be positioned accurately. By counting the number of ultrasonic fringes that pass while rotating the object, one can measure an angular position change in tenths of degrees. This can be very useful in situations where an accurate positioning is required, but a direct angle measurement is not feasible. This idea is similar to the way in which Fabry–Perot interferometers are used in optics to position objects linearly accurately, except that it is being done here for angular positioning with a wavelength that is more practical for many applications such as robotics. For example, a 40kHz ultrasonic source can be used to position objects as accurately as 0.1°. This accuracy can be enhanced by using a source with a higher frequency.

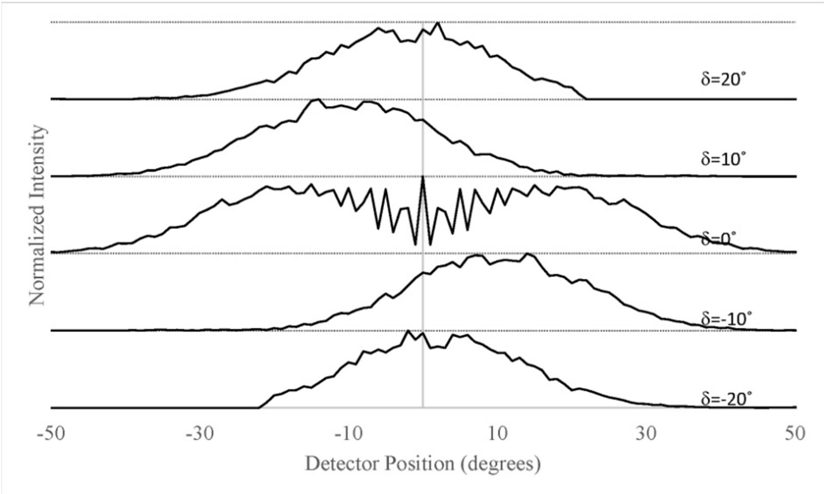

(a) Time integrated intensity *vs*. angular detector position of a reflection from 135° corner twisted by an angle δ. $\delta = 0$ means that the incident pulse direction divides the corner into halves.

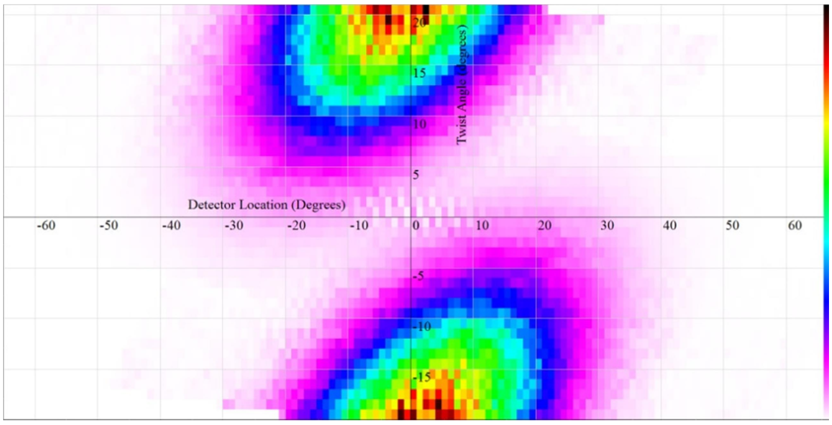

(b) A large set of curves, such as those in Fig. 9a, packed in a single 3D plot. X-axis: detector location in degrees. Y-axis: twist angle in degrees. The normalized intensity is represented by the color scale to the right of each figure.

FIG. 9. Effect of changing a 135° corner pointing direction on the reflected wavefront shape.

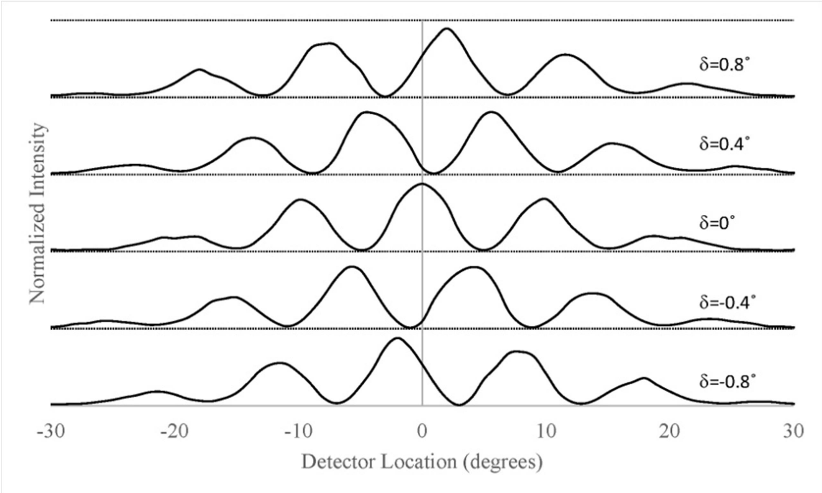

(a) Time-integrated intensity *vs*. angular detector position of a reflection from 169° corner twisted by an angle δ. δ = 0 means that the incident pulse direction divides the corner into halves.

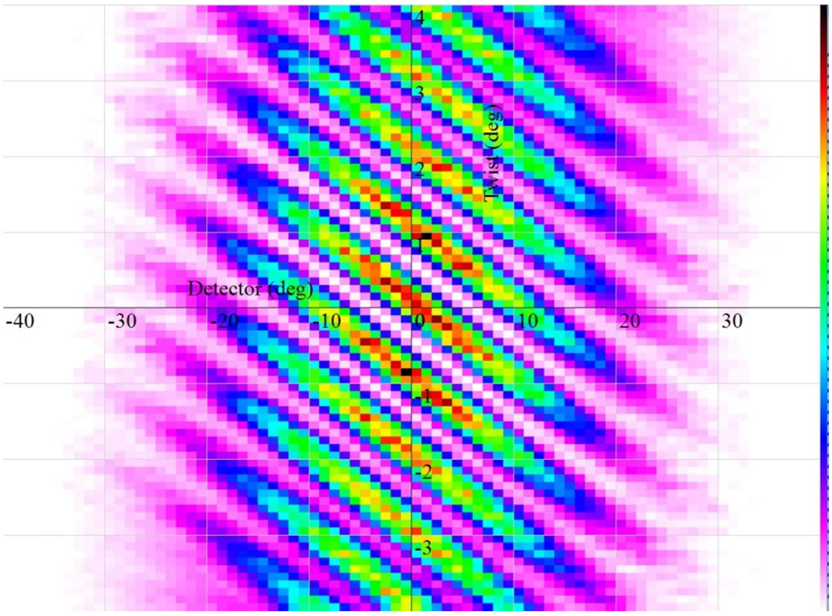

(b) A large set of curves, such as those in Fig. 10a, packed in a single 3D plot. X-axis: detector location in degrees. Y-axis: twist angle in degrees. The normalized intensity is represented by the color scale to the right of each figure.

FIG. 10. Effect of changing a 169° corner pointing direction on the reflected wavefront shape.

Seeing Behind a Corner

Observing changes in the reflected wavefront properties is not limited to objects with a direct line of sight. An object hidden behind a corner can still be detected by analyzing the waves reflected from an adjacent wall. To demonstrate this, Figs. 12a and 12b show the echoes coming out of empty hallways that are 150 *cm* and 200 *cm* long, respectively. The outgoing pulse source is placed close to the entrance without having a direct line of sight into it. The time-spacing and number of wavefronts in the train of echoes coming out gives the hallway depth and width. A robot with a digital signal processor (DSP) can detect these simple features and guess the shape of that environment after getting some artificial intelligence training.

Objects in real life do not always have simple geometries. However, a given object will change a reflected pulse in a specific way. In other words, a complicated object will have its signature in the reflected wavefronts. To demonstrate this, an object that consists of two overlapping squares with one of them rotated 45° is placed inside the 200 *cm* long hallway. The reflections coming out, after placing the object 100 *cm* and 150 *cm* inside the hallway, are shown in Figs. 13a and 13b, respectively. Note that the signature of the unseen object, marked in the figures, is the same for both cases. Note also how the echoes that are a characteristic of the hallway itself at the upper left corner of Fig. 12b are still there in Fig. 13. One can get the information about the object itself and still get the hallway dimensions.

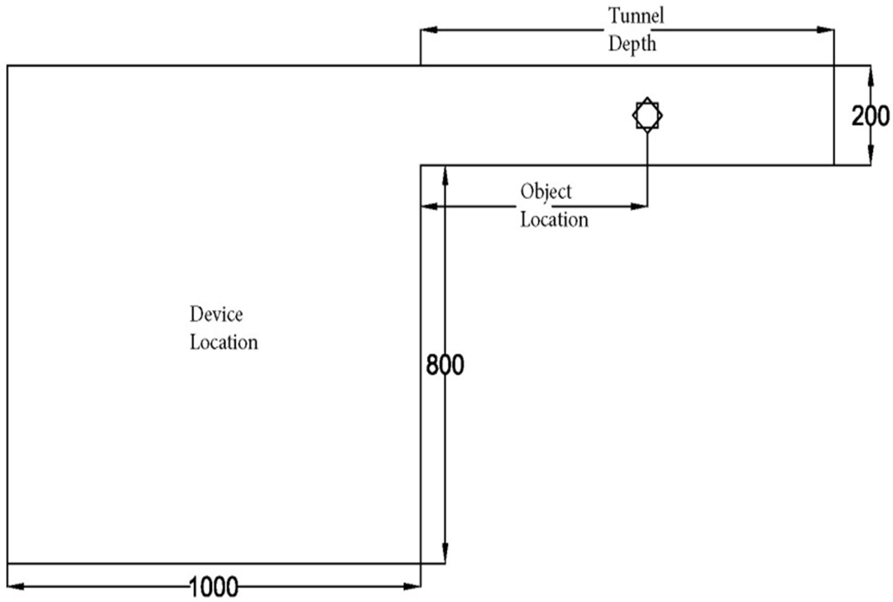

FIG. 11. Environment walls used to collect the simulated data shown in Figs. 12 and 13.

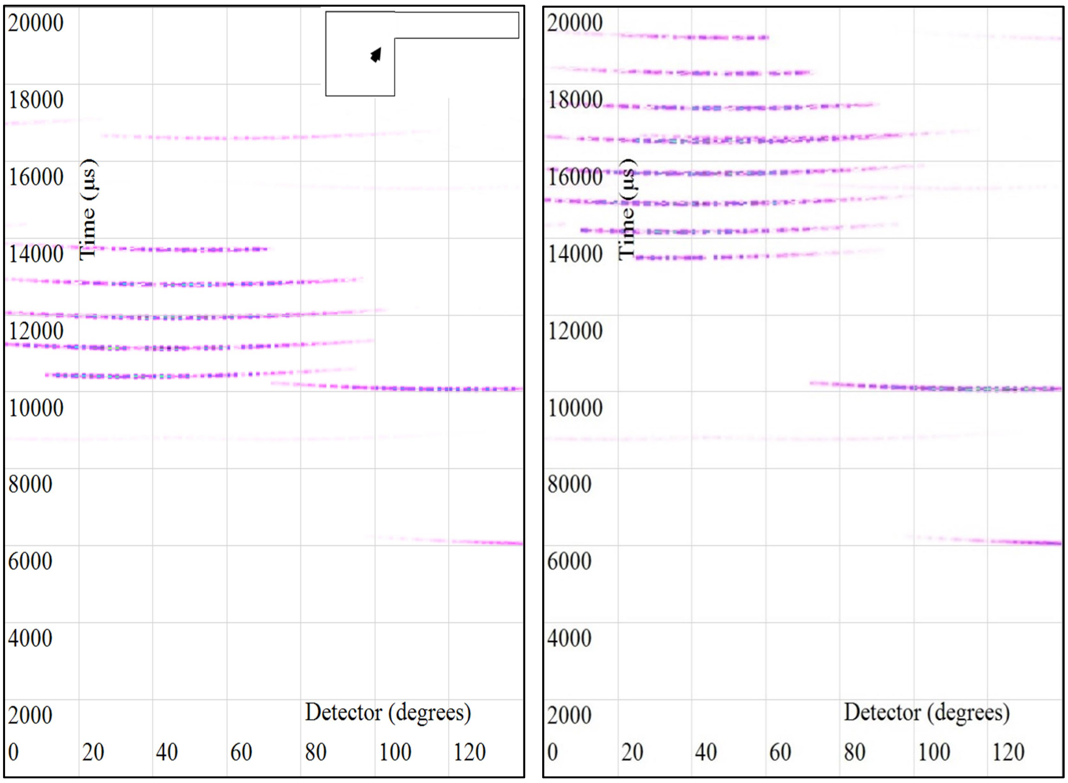

(a) Echoes coming out of a 150 *cm* deep hallway. (b) Echoes coming out of a 200 *cm* deep hallway.

FIG. 12. Train of echoes coming out of a hallway, after emitting a pulse into it, without a direct line of sight into the hallway. The inset at the upper right corner of Fig. 12a describes the geometry of the walls under study. The test environment is similar to the one shown in Fig. 11, but without the test object placed inside the tunnel.

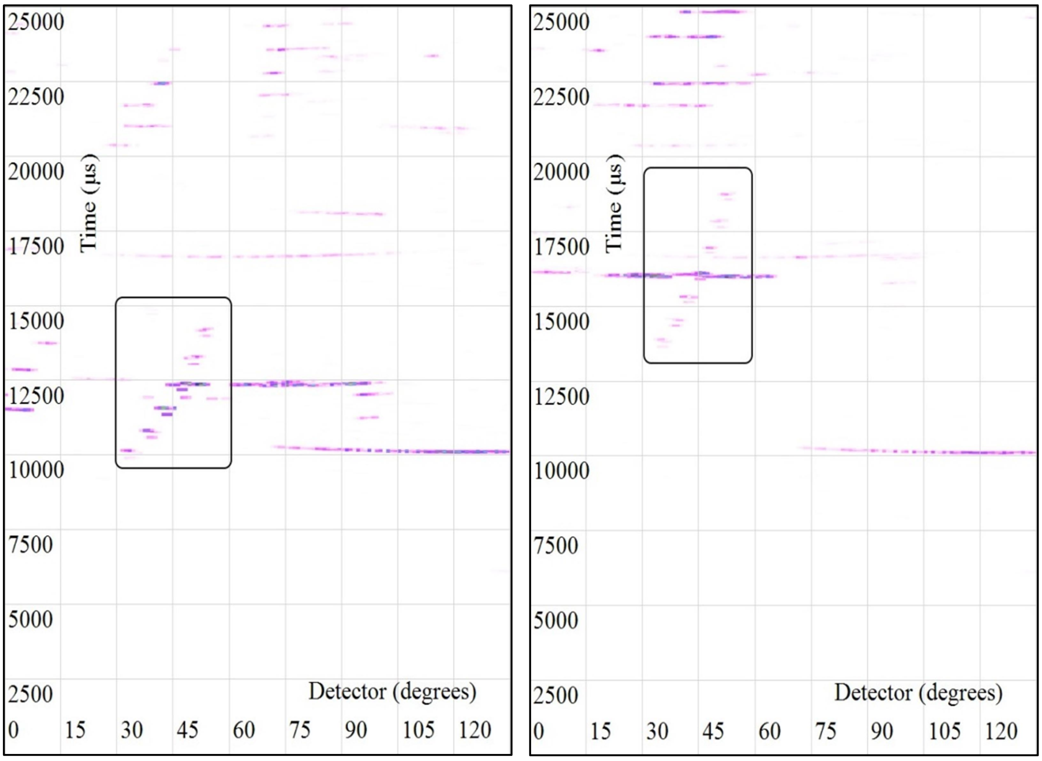

(a) Object placed 150 *cm* inside a hallway. (b) Object placed 200 *cm* inside a hallway.

FIG. 13. Signature of an object that consists of two overlapping squares with one of them rotated 45°, placed inside a hallway, without a direct line of sight. Test environment design is shown in Fig. 11.

Conclusion

In this paper, a new method for mapping an environment and discovering unseen objects is demonstrated. This was achieved by sending a pulse with a known shape and listening to the reflections from all directions in real time. The changes in the shape of the reflected wavefronts enable detecting simple features, such as a slope, an angle or a twist in a corner. The ability to measure object rotation, with an accuracy as high as 0.1°, by counting ultrasound interference fringes and the ability to discover unseen objects behind a corner, are demonstrated.

References

[1] Hinderer, M., Friedrich, P. and Wolf, B., Robotics and Autonomous Systems, 94 (2017) 219.

[2] Dairi, A., Harrou, F., Senouci, M. and Sun, Y., Robotics and Autonomous Systems, 100 (2018) 287.

[3] Padgett, J. and Campbell, M., Robotics and Autonomous Systems, 98 (2017) 292.

[4] Urena, J., Mazo, M., Garcıa, J.J., Hernandez, A. and Bueno, E., Robotics and Autonomous Systems, 29 (4) (1999) 269.

[5] Martınez, M. and Benet, G., Sensors, 10 (12) (2010) 10683.

[6] Benet, G., Martınez, M., Blanes, F., Perez, P. and Sim´o, J.E., Robotics and Autonomous Systems, 50 (1) (2005) 13.

[7] Popelka, M., Struska, J. and Struska, M., International Journal of Circuits, Systems and Signal Processing, 10 (2016) 82.

[8] Christopher, T. C., M.A. Thesis, University of Illinois at Urbana-Champaign, (2012), USA.

[9] Ding, T., Hu, H., Bai, C., Guo, S., Yang, M., Wang, S. and Wan, M., Ultrasonics, 69 (2016) 166.

[10] Khan, M.A., Jilani, S.Z., Menouar, H. and Al-Majed, A.A., Ultrasonics, 39 (5) (2001) 321.

[11] Ding, T., Zhang, S., Fu, Q., Xu, Z. and Wan, M., Ultrasonics, 54 (1) (2014) 147.

[12] Woodward, B. and Sharp, H., Ultrasonics, 29 (5) (1991) 381.

[13] Zelenyak, A.-M., Schorer, N. and Sause, M.G.R., Ultrasonics, 83 (2018) 103.

[14] Boltryk, P., Hill, M., Keary, A., Phillips, B., Robinson, H. and White, P., Ultrasonics, 42 (1-9) (2004) 473.

[15] Gao, W. and Hinders, M.K., Robotics and Autonomous Systems, 53 (2) (2005) 89.

[16] Dokmanic, I., Parhizkar, R., Walther, A., Lu, Y.M. and Vetterli, M., Proceedings of the National Academy of Sciences, 110 (30) (2013) 12186.

[17] Dokmanic, I., Lu, Y.M. and Vetterli, M., In: Acoustics, Speech and Signal Processing (ICASSP), IEEE, (2011) 321.

[18] Crocco, M., Trucco, A., Murino, V. and Del Bue, A., In: Signal Processing Conference (EUSIPCO), Proceedings of the 22nd European IEEE, (2014) 910.

[19] Lazik, P., Rajagopal, N., Shih, O., Sinopoli, B. and Rowe, A., In: Proceedings of the 13th ACM Conference on Embedded Networked Sensor Systems, ACM, (2015) 73.

[20] Shih, O. and Rowe, A., In: Proceedings of the ACM/IEEE Sixth International Conference on Cyber-Physical Systems, ACM, (2015) 149.

[21] Al-Shorman, M. and Al-Kofahi, M., International Journal of High-performance Computing Applications, 33 (5) (2019) 1019.